Geophysical Research Letters

RESEARCH LETTER
10.1029/2021GL094405

Parameterizing Eddy Transport of Biogeochemical Tracers

Channing J. Prend[1], Glenn R. Flierl[2], Katherine M. Smith[3], and Alexis K. Kaminski[4]

[1]University of California San Diego, Scripps Institution of Oceanography, La Jolla, CA, USA, [2]Department of Earth, Atmospheric, and Planetary Sciences, Massachusetts Institute of Technology, Cambridge, MA, USA, [3]Los Alamos National Laboratory, Los Alamos, NM, USA, [4]Department of Mechanical Engineering, University of California Berkeley, Berkeley, CA, USA

Key Points:

- For nutrient-phytoplankton systems, cross-diffusion can be important to the parameterized eddy flux of either variable
- For reactive tracers, the validity of eddy diffusion parameterizations also relies on timescale separation between the reaction and eddies
- This timescale separation is violated for biological processes at the submesoscale, which can help explain biases in climate models

Supporting Information:

Supporting Information may be found in the online version of this article.

Correspondence to:

C. J. Prend,
cprend@ucsd.edu

Citation:

Prend, C. J., Flierl, G. R., Smith, K. M., & Kaminski, A. K. (2021). Parameterizing eddy transport of biogeochemical tracers. *Geophysical Research Letters*, *48*, e2021GL094405. https://doi.org/10.1029/2021GL094405

Received 19 MAY 2021
Accepted 5 OCT 2021

Abstract The distribution of oceanic biogeochemical tracers is fundamentally tied to physical dynamics at and below the mesoscale. Since global climate models rarely resolve those scales, turbulent transport is parameterized in terms of the large-scale gradients in the mean tracer distribution and the physical fields. Here, we demonstrate that this form of the eddy flux is not necessarily appropriate for reactive tracers, such as nutrients and phytoplankton. In an idealized nutrient-phytoplankton system, we show that the eddy flux of one tracer should depend on the gradients of itself and the other. For certain parameter regimes, incorporating cross-diffusion can significantly improve the representation of both phytoplankton and nutrient eddy fluxes. We also show that the efficacy of eddy diffusion parameterizations requires timescale separation between the flow and reactions. This result has ramifications for parameterizing subgrid scale biogeochemistry in more complex ocean models since many biological processes have comparable timescales to submesoscale motions.

Plain Language Summary Tiny algae called phytoplankton play a key role in marine food webs and oceanic uptake of carbon dioxide. Therefore, determining the distribution of phytoplankton is necessary to model marine ecosystems and the global carbon cycle accurately. These organisms, and the nutrients they need to grow, are moved around by turbulent motions in the ocean. However, most climate models do not capture the small-scale eddies that help determine patterns in phytoplankton biomass. Instead, the models use mathematical approximations to indirectly estimate the transport of phytoplankton by these turbulent processes. In this study, we use idealized numerical simulations to show that the commonly used approximation method may not correctly characterize the eddy transport of phytoplankton in many cases. This result can be used to help improve the representation of phytoplankton in more complex models, which are used to predict future climate.

1. Introduction

Biogeochemical properties in the ocean, including nutrients and phytoplankton, exhibit patchiness at the mesoscale and submesoscale (Lévy & Martin, 2013; Mahadevan & Campbell, 2002; Martin et al., 2002). This is evident from satellite images of ocean color, a proxy for phytoplankton biomass, which clearly show the expression of eddies, filaments, and other small-scale structure in the flow (Gower et al., 1980). Phytoplankton patchiness is generated by a complex interplay between physical and biogeochemical processes, each with their own range of length and time scales (Flierl & McGillicuddy, 2002; Lévy et al., 2012; McGillicuddy, 2016). This includes the lateral stirring of large-scale gradients by the turbulent flow (Abraham, 1998; Martin, 2003; McKiver et al., 2009) as well as stimulation of phytoplankton growth by (sub-)mesoscale processes delivering nutrients to the euphotic zone (Falkowski et al., 1991; Flierl & Davis, 1993; Freilich & Mahadevan, 2019; Lévy et al., 2001; Uchida et al., 2020).

The relative importance of stirring, which passively reorganizes existing gradients, versus localized upwelling, which actively forces changes in phytoplankton abundance, must be determined in order to quantify the global significance of (sub-)mesoscale productivity (Lévy et al., 2018). Still, it has been suggested that phytoplankton patchiness impacts large-scale productivity (Brentnall et al., 2003; Jenkins, 1988) and may be important to global biogeochemical budgets (Doney et al., 2004; Falkowski et al., 1991; Omand et al., 2015; Platt & Sathyendranath, 1988). This poses a problem for global climate models, which rarely

resolve processes at or below the mesoscale, $\mathcal{O}(100\text{km})$. Therefore, the tracer transport associated with the unresolved dynamics must be parameterized. This is typically done by assuming that eddy fluxes are proportional to the gradients in the mean field, the so-called gradient-diffusion hypothesis. In this framework, the unresolved turbulent dispersion is represented as an enhanced molecular diffusion:

$$\overline{u'c'} = -K_e \nabla \bar{c} \tag{1}$$

where K_e is an effective diffusivity, c is any arbitrary tracer, the overbar represents an ensemble average and the prime denotes time-dependent fluctuations from the mean. The implicit assumption is that the chaotic random motions associated with turbulence are comparable to Brownian motion. Despite its near-ubiquitous use, limitations of the eddy-diffusion parameterization have been noted (Ferrari & Nikurashin, 2010; Lee et al., 1997; Manucharyan et al., 2017; Sobel, 1999), particularly for reactive tracers, which have a growth or decay in time that is independent of the flow and thus do not remain constant following a fluid parcel.

Many biogeochemical quantities can be modeled as reactive tracers. For example, phytoplankton growth via nutrient uptake and loss due to zooplankton grazing can be expressed mathematically as reaction terms. The reaction timescale of a tracer is known to impact both the degree of observed patchiness (Mahadevan & Campbell, 2002), as well as the validity of eddy diffusion parameterizations (Pasquero, 2005). Indeed, assessing the ability of the gradient-diffusion hypothesis, Equation 1, to accurately represent the transport of both reactive and nonreactive tracers is not a new concept (da Silva & Pereira, 2007; Lightstone & Raithby, 2009; Mooney & Wilson, 1993). However, the past work that approaches this problem in the context of oceanic biogeochemical tracers typically either (a) uses relatively complex biogeochemical models coupled to idealized background flows (Abraham, 1998; Denman, 2003; Tzella & Haynes, 2007) or (b) uses nonreactive tracers in realistic flows (Smith et al., 2016). These approaches, while useful, are computationally expensive and it can be challenging to isolate the fundamental dynamics. Here, we argue that there is still insight to be gained from a system with a simple biogeochemical model and flow field. This allows us to investigate the theoretical underpinnings of the physical-biological interactions and examine the system across the full range of parameter space. The results can then inform past and future work that employs more complex models, both physical and biogeochemical.

2. Methods and Theory

2.1. Biological Model

Nutrient-phytoplankton-zooplankton (NPZ) models have been used in oceanographic research for decades. A standard NPZ model has five transfer functions, each with countless possible functional forms (see Franks, 2002 for a nice review). The NPZ framework has also been extended to include the effects of bacteria and detritus, and is similar to the multicomponent systems used in the current generation of global climate models (Aumont et al., 2015; Cushing, 1975; Fasham et al., 1990). However, a more complex biogeochemical model is not necessarily a better one for developing process-based understanding (Franks, 2002; Turner et al., 2014). Here, we follow the lead of Hodges and Rudnick (2004), and Freilich and Mahadevan (2019), and opt to ignore the zooplankton component entirely, selecting basic Lotka-Volterra forms for the remaining transfer functions. The result is the simplest possible model that still captures fundamental aspects of plankton dynamics. Including explicit diffusion (with diffusivity κ) the equations are:

$$\frac{\partial N}{\partial t} + \mathbf{u} \cdot \nabla N - \kappa \nabla^2 N = -\mu N P - \lambda N + \lambda N_D \tag{2}$$

$$\frac{\partial P}{\partial t} + \mathbf{u} \cdot \nabla P - \kappa \nabla^2 P = \mu N P - \lambda P, \tag{3}$$

where the nutrient (N) and phytoplankton (P) concentration fields have the same units (e.g., moles of nitrogen per unit volume), μ ($[\text{mol N m}^{-3}]^{-1}\text{s}^{-1}$) is the nutrient uptake rate, λ $[\text{s}^{-1}]$ is the entrainment rate, and $\mathbf{u}$ is a 2-dimensional velocity field. These equations describe the dynamics of the biology in the upper ocean, where N and P represent average concentrations in the mixed layer, and N_D is the subsurface nutrient concentration. The right-hand side reaction terms in Equation 2 correspond to nutrient depletion via

uptake by phytoplankton ($-\mu N P$) and detrainment across the mixed-layer base ($-\lambda N$), as well as nutrient resupply by the entrainment of nutrient-rich waters from below (λN_D). Although we suggest that λ can be interpreted as an entrainment rate, it is specified a priori and not related to the velocities. Technically, λ acts like a reaction rate from the perspective of the biological system. Analogous reaction terms are present in Equation 3, with the exception that entrainment only decreases P (since it is assumed that subsurface waters below the mixed layer are also below the euphotic zone and thus devoid of phytoplankton). This system can be nondimensionalized in terms of the following dimensionless variables:

$$x^* = \frac{x}{L}, \quad y^* = \frac{y}{L}, \quad \mathbf{u}^* = \frac{\mathbf{u}}{U}, \quad t^* = t\mu\tilde{N}_D, \quad N^* = \frac{N}{\tilde{N}_D}, \quad P^* = \frac{P}{\tilde{N}_D}, \tag{4}$$

where $\sim N_D$ is some characteristic N value, for example, $\langle N_D \rangle$ where $\langle \cdot \rangle$ denotes a spatial average. The diffusive terms in Equations 2 and 3 scale inversely with the Péclet number, $Pe = UL/\kappa$. The entire right-hand side of both equations scale with the Damköhler number, $Da = \mu\tilde{N}_D L/U$, which is the ratio of advective (L/U) and reactive ($1/\mu\tilde{N}_D$) timescales. The entrainment terms are further scaled by the ratio of reaction rates ($\lambda/\mu\tilde{N}_D$). See Text S1 in Supporting Information S1 for the full nondimensional equations.

Our motivation in choosing this simplified set of equations is to avoid introducing extraneous nonlinearity, for example, from poorly constrained transfer functions associated with the zooplankton component in NPZ models. Certainly, we note that this system does not capture all of the relevant processes controlling phytoplankton biomass. By neglecting zooplankton, our model does not capture top–down controls, which have been shown to be important in determining phytoplankton abundance (Behrenfeld & Boss, 2014); these predator-prey interactions are also thought to be influenced by the dominant scales of motion in the flow (Richards & Brentnall, 2006; Srokosz et al., 2003; Taniguchi et al., 2014). The advantage of our idealized formulation, Equations 2 and 3, is that it is a tractable system which can be probed to understand the sensitivity to various parameters. Our reduced NPZ form allows us, for example, to conduct a multiple scale analysis, which provides theoretical insight into the appropriate form of reactive tracer eddy fluxes.

The concept of an eddy diffusivity introduced by Taylor (1921) is related to the Lagrangian velocity experienced by particles. However, this framework can be extended to the spreading of tracers in an Eulerian context. Papanicolaou and Pironneau (1981) showed that by assuming a scale separation between the eddies and mean flow, Equation 1 can be derived via a multiple scale analysis of the advection-diffusion equation for a passive tracer. Here, we apply a similar technique to Equations 2 and 3 to illustrate how additional reaction terms influence the form of the eddy flux. As in the passive tracer case, we assume a scale separation between the turbulent eddies (ℓ) and the large-scale circulation (L). This suggests a perturbation expansion in terms of the small parameter $\epsilon \equiv \ell/L$, where slow time and space variables are defined as $T = \epsilon t$ and $\mathbf{X} = \epsilon \mathbf{x}$, respectively. The velocity is also decomposed into mean and eddy components, $\mathbf{u} = \mathbf{U}(\mathbf{X}, T) + \mathbf{u}'(\mathbf{x}, t;\ \mathbf{X}, T)$. Solutions for N and P then take the form:

$$N = N_0(\mathbf{X}, T) + \epsilon N_1(\mathbf{x}, t; \mathbf{X}, T) + \mathcal{O}(\epsilon^2) \tag{5}$$

$$P = P_0(\mathbf{X}, T) + \epsilon P_1(\mathbf{x}, t; \mathbf{X}, T) + \mathcal{O}(\epsilon^2). \tag{6}$$

Note that the mean flow and leading order biological behavior are both taken to be functions of the large scales only. We substitute the expansions, Equations 5 and 6, into the advection-diffusion-reaction system, Equations 2 and 3. At each order of ϵ, averaging over the small and fast scales yields a solvability condition. The evolution equations for the large-scale, long-time, averaged tracer concentrations, $\bar{N}$ and $\bar{P}$, are then obtained by summing the solvability conditions up to $\mathcal{O}(\epsilon^2)$. The results (see Text S2 in Supporting Information S1 for details, and Flierl and McGillicuddy (2002), which uses a cruder approximation for the physics) imply that the eddy fluxes of N and P have the form:

$$\overline{u'N'} = -K_{NP}\nabla\bar{P} - K_{NN}\nabla\bar{N}, \tag{7}$$

$$\overline{u'P'} = -K_{PP}\nabla\bar{P} - K_{PN}\nabla\bar{N}, \tag{8}$$

where K_{NP}, K_{NN}, K_{PP}, are K_{PN} are effective diffusivities that can be expressed in terms of μ, λ, and $\bar{P}$ (see Text S4 in Supporting Information S1). Equations 7 and 8 have the eddy fluxes (i.e., the magnitude of the vectors $|\langle \mathbf{u}'P' \rangle|$ and $|\langle \mathbf{u}'N' \rangle|$) depending on the large-scale, mean tracer gradients ($|\nabla\langle P \rangle|$ and $|\nabla\langle N \rangle|$), as in

the traditional gradient-diffusion result. However, unlike in the passive tracer case, we find that the fluxes of N and P depend on the large-scale gradients of both tracers. There may be cases, for example, where the eddy flux of phytoplankton is controlled by the gradient in the mean nutrient concentration (rather than by gradients in $\bar{P}$). This phenomenon is known as cross-diffusion (Vanag & Epstein, 2009) and is due to the coupling between Equations 2 and 3 that results from the nonlinear uptake term, $\mu N P$.

To understand cross-diffusion physically, consider a case where $\langle N \rangle$ increases to the north. A parcel of fluid moving south will have a positive N'; as a result P' will increase. When it arrives at some latitude, it will have positive P' and negative v'. Likewise, a parcel coming from the south will arrive at the same latitude with negative P' and positive v'. Thus, the flux $\langle v' P' \rangle$ is negative, corresponding to a P flux down the gradient of $\langle N \rangle$. There can, of course, also be contributions from the gradient of $\langle P \rangle$, but, for linearized perturbation equations, the two contributions can be treated separately and added to get the net flux. The diffusive coefficients associated with the cross terms can also be negative. For example, consider an infinitesimal wave on a background with uniform μ, λ and no gradient in nutrients. Flows away from high subsurface nutrients carry excess phytoplankton, which draws down nutrients producing a negative anomaly, while flow the other way has a positive anomaly. In other words, although there is no background gradient in nutrients, there is a nutrient flux up the gradient of phytoplankton.

2.2. Physical Model

With the results from the multiple scale analysis in mind, we now investigate the dynamics of the nutrient-phytoplankton model in a simple flow field. The dimensional Equations 2 and 3 are coupled to a 2-D stirring flow adapted from the clever "renovating wave" model in Pierrehumbert (1994). The velocity fields are generated by a stream function of the form:

$$\Psi = \sum_{n=1}^{4} U_n \cos(k_{1n} x + k_{2n} y + \theta_n), \tag{9}$$

where the wavenumbers k_{1n} and k_{2n} and amplitude U_n are selected so that the kinetic energy spectrum is consistent with scaling laws of turbulence (i.e., $k^{-5/3}$ slope) and θ_n is a random-walking phase shift. In other words, sinusoidal shear flows are periodically "renovated" by a random phase shift at each time step ($dt = 1/32$ to satisfy a Courant-Friedrichs-Lewy condition) to generate a flow that is zero-mean in time and has qualitative similarities to 2-D turbulence. We tested multiple spectra, including a nonlocal k^{-3} spectrum, but opted for a flow with more small-scale energy, since this is common in surface quasi-geostrophic turbulence characteristic of the upper ocean. The exact choice of spectrum does not affect the existence of the cross-fluxes or the dependence on the relative time scales. Similar models have been used in the study of phytoplankton patchiness (Hodges & Rudnick, 2006; Young et al., 2001). The model domain is $4\pi \times 4\pi$ and doubly periodic. N and P transport is represented by a first-order upwind advection scheme to maintain positivity. The flow is homogeneous by construction and nearly isotropic (it is not exactly isotropic due to the double periodicity), so it can be represented by a single constant diffusivity.

2.3. Model Parameters

In principle, μ, λ, and N_D could all be spatially variable. Here, we describe simulations in which μ is modeled as a sinusoid, $\mu_0 + \mu_1 \cos(y/2)$. This form is chosen to maintain periodicity. The N_D and initial distribution of total nitrogen in the system ($S = N + P$) are also selected to be sinusoidal, although with east-west gradients to distinguish from gradients in μ; λ is chosen to be a constant. The motivation for selecting μ and N_D to be orthogonal is to create gradients in N and P which are distinctly different, allowing us to more easily investigate the cross fluxes. The initial P distribution is determined from the leading order P solution found in the multiple scale analysis ($P_0 = N_D - \lambda/\mu$). The initial N distribution is determined by subtracting P_0 from the initialized S ($N_0 = S_0 - P_0$). The initial conditions are plotted in Figure S1 in Supporting Information S1. Eddies and filaments in the N and P fields quickly form, and are maintained, in many cases, through biological reactions. Figure 1 shows snapshots of the nutrient and phytoplankton concentration fields (a, b) and nutrient and phytoplankton eddy fluxes (c, d) for two different simulations after reaching equilibrium. The patchy, filamentary distributions in Figure 1a are representative of many oceanic regimes.

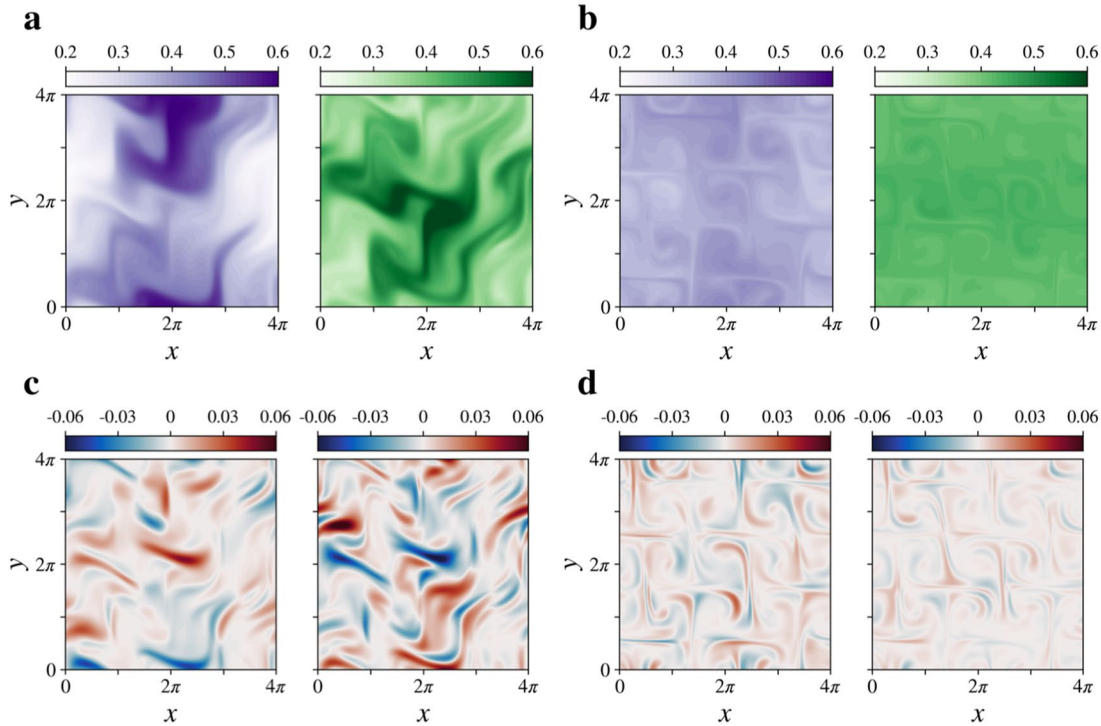

Figure 1. Snapshot at $t = 1{,}000$ of nutrient (purples) and phytoplankton (greens) concentrations (a), (b) as well as nutrient (left) and phytoplankton (right) eddy fluxes (c), (d) for two simulations with the same flow field but varied reaction rates, (a), (c) $\lambda = 0.03$, $\langle\mu\rangle = 0.08$, $Da = 1$ and (b), (d) $\lambda = 0.003$, $\langle\mu\rangle = 0.008$, $Da = 0.1$.

The simulations have the same flow field and initial conditions but varied reaction rates, namely $Da = 1$ for Figures 1a and 1c and $Da = 0.1$ for Figures 1b and 1d. Mean fields for these simulations are plotted in Figure S2 in Supporting Information S1. Parameter choices for all the different experiments in this study are given in Table S1 in Supporting Information S1.

3. Results

The long-time behavior of the model is greatly affected by the presence of reaction terms as well as the reaction timescales. To illustrate this, several simulations were run with different values of λ and $\langle\mu\rangle$. Figure 2 shows time series of phytoplankton concentration and variance for different values of Da, which is diagnosed from the dimensional model using the spatial averages $\langle\mu\rangle$, $\langle N_D\rangle$, and $\sqrt{\langle u^2\rangle}$. For a nonreactive tracer (i.e., $Da = 0$) the mean tracer concentration over the domain stays constant and the variance decays exponentially to zero as the stirring smooths out the gradients associated with the initial conditions (Hodges & Rudnick, 2006; Pierrehumbert, 2000). Biological reaction terms introduce a chaotic time dependence. After an initial transient period, the mean tracer concentration fluctuates randomly in time around an equilibrium level which depends on the relative rates of phytoplankton growth and losses. When the ratio of phytoplankton detrainment to growth, $\lambda/\langle\mu\rangle$, is held constant, the equilibrium concentration value is fixed. Fluctuations are also seen in the tracer variance, which never decays to zero. The amplitude of the changes in $\langle P\rangle$ depends on the ratio of reaction and flow timescales, Da. The fluctuations (and consequently the variance) are largest for $Da = 1$ and $Da = 10$ due to the interaction between stirring and growth. This can be seen from the snapshots of N and P in Figure 1; the tracers are well-mixed in 1b ($Da = 0.1$) compared to 1a ($Da = 1$).

The presence of biological reactions impacts the appropriate value of the effective diffusivity (see Figure S3 and Text S3 in Supporting Information S1), as well as the validity of the gradient-diffusion hypothesis. Since the time-mean of the velocity field is zero, the tracer fluxes from the model advection scheme are equal to the eddy fluxes $\overline{u'P'}$ and $\overline{u'N'}$, taken to be the magnitude of the vectors $|\langle \mathbf{u}'P'\rangle|$ and $|\langle \mathbf{u}'N'\rangle|$. Note

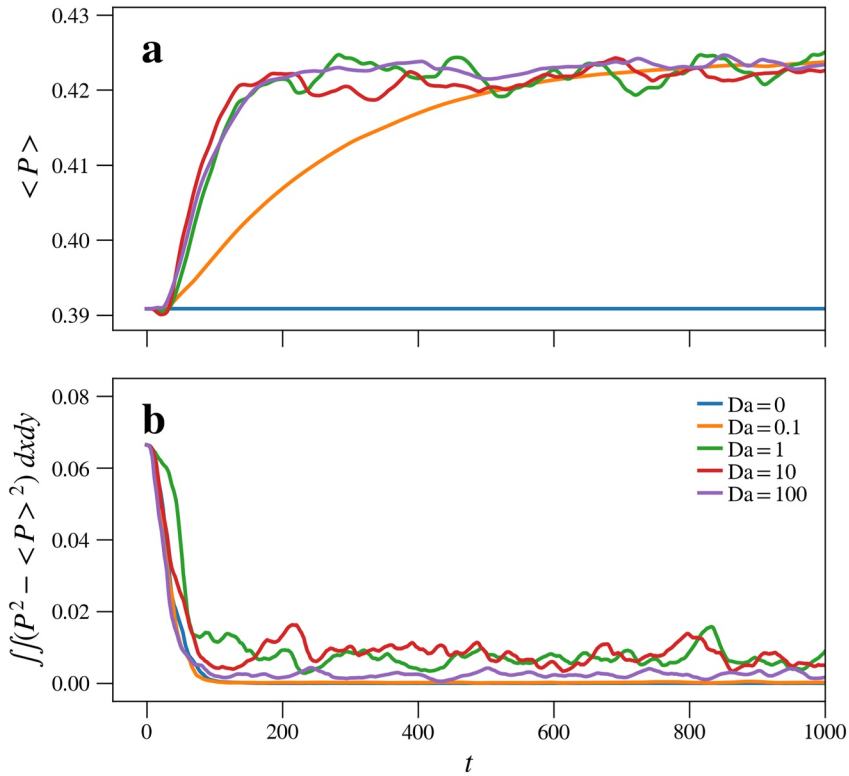

Figure 2. Time series of (a) Mean phytoplankton concentration, and (b) Phytoplankton concentration variance integrated over the domain. Plotted for five simulations with the same initial conditions and flow field but varied *Da*.

that here, eddy flux refers to the advective transport of tracers by the fluctuating component of the velocity field, rather than the biological fluxes (i.e., $N'P'$ terms), often called eddy reactions. While eddy reactions also affect the distribution of biogeochemical tracers, their magnitude depends inherently on the mathematical form of the reaction terms. For our highly simplified model, the eddy reactions are much smaller than the eddy transports, although this is not necessarily the case in more complex biological models (Lévy & Martin, 2013).

Since we are focused on transport by the time-fluctuating velocity, the advective fluxes diagnosed directly from the model are referred to as the "true" eddy flux. These are depicted, for example, at a single time step in Figures 1c and 1d. An effective diffusivity, K_e can be computed by regressing the true eddy flux onto the tracer gradients, $|\nabla\langle P\rangle|$ and $|\nabla\langle N\rangle|$, calculated at each grid cell from the mean N and P distributions after the simulation reaches equilibrium ($t = 1000$) to the end of the run ($t = 5000$). It is then possible to compare the true eddy flux with $-K_e\nabla i$ at each grid point. Figure 3 gives examples of this for two simulations with the same initial conditions, one with biological reaction terms (Figure 3a) and one without (Figure 3b). Deviations from the black 1:1 line indicate a breakdown of the standard gradient-diffusion hypothesis.

Figure 3 suggests that, for the same initial conditions and velocity field, reactive tracer transport is poorly represented in terms of an eddy diffusion when compared to the nonreactive tracer case. Naturally, however, the specifics will depend on the model parameters. To illustrate this, we calculate the R^2 value, which measures the goodness of fit, to quantify the validity of $\overline{u'c'} = -K_e\nabla i$ for different values of *Da*. R^2 values near 1 suggest that the gradient-diffusion hypothesis is a good assumption, whereas smaller R^2 values indicate that it breaks down. The results in Section 2.1 point to the possible importance of cross-diffusion, so we also compute K_{NP}, K_{NN}, K_{PP}, and K_{PN} by regressing the true eddy fluxes onto both $\nabla\bar{P}$ and $\nabla\bar{N}$, rather than regressing $\overline{u'P'}$ onto $\nabla\bar{P}$ only (and $\overline{u'N'}$ onto $\nabla\bar{N}$ only). Adding additional predictors to a regression model can lead to spurious increases in R^2, so adjusted R^2 values (Cramer, 1987) are calculated for the multiple regression (see Text S4 in Supporting Information S1).

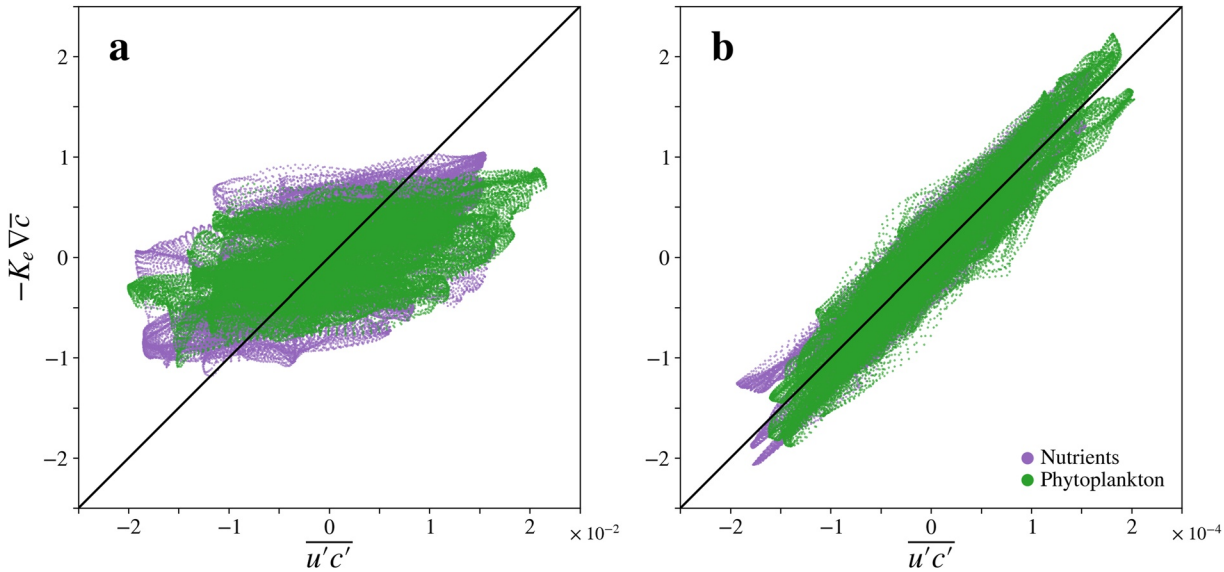

Figure 3. (a) Calculated eddy fluxes of N (purple) and P (green) from $\nabla\iota$ and least squares fitted K_e versus the diagnosed eddy fluxes at each grid cell for a simulation with biological reaction terms ($\lambda = 0.03, \langle\mu\rangle = 0.08$), and (b) For the same initial conditions but with reaction rates λ and $\langle\mu\rangle$ set to 0 (i.e., N and P are nonreactive tracers).

R^2 is found to vary strongly with Da (Figure 4 and Figure S4 in Supporting Information S1). Since reaction terms scale with Da in the nondimensionalized N and P equations, they are negligible in the limit of slow reaction rates relative to stirring, $Da \ll 1$. Consequently, in these regimes, N and P can be treated as nonreactive tracers and have high R^2 values (>0.7), both for $\overline{u'P'} = -K_e \nabla \bar{P}$ (blue in Figure 4) and $\overline{u'P'} = -K_{PP} \nabla \bar{P} - K_{PN} \nabla \bar{N}$ (orange in Figure 4). Still, even passive tracer transport is not perfectly described by an eddy diffusion, which may be related to nonlocal effects (Lee et al., 1997; Manucharyan et al., 2017; Sobel, 1999). When the reaction and flow timescales are of the same order, $Da \sim \mathcal{O}(1)$, R^2 values are much lower (<0.3), suggesting a breakdown of the gradient-diffusion hypothesis. We note that this is true even when cross-diffusion terms are included. Recall that the derivation of Equations 7 and 8 required space and time-scale separation between the turbulent eddies and reactions. This assumption is violated, by definition, when $Da \sim \mathcal{O}(1)$. In other words, mimicking turbulent transport as an enhanced diffusion is only valid when there is a timescale separation between the reaction and eddies. We also find that when $Da \sim \mathcal{O}(1)$, fluctuations in N and P persist over the scales of variation of $\bar{P}$, $\bar{N}$, μ, and N_D, and tend to be out

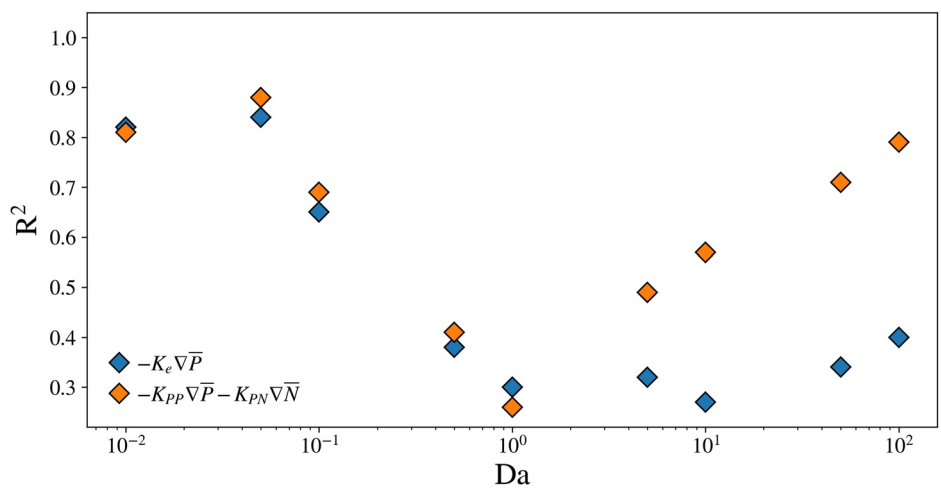

Figure 4. R^2 of the parameterized eddy flux and true eddy flux as a function of Da assuming $\overline{u'P'} = -K_e \nabla \bar{P}$ (blue) and $\overline{u'P'} = -K_{PP} \nabla \bar{P} - K_{PN} \nabla \bar{N}$ (orange).

of phase with the flow (Text S2 in Supporting Information S1), which likely contribute to the breakdown of the parameterization.

In the limit of fast reaction rates relative to stirring, $Da \gg 1$, the R^2 values are significantly increased by including cross-diffusion (Figure 4). This suggests that there are parameter regimes where the mean nutrient gradient is a better predictor of the phytoplankton eddy fluxes than the mean phytoplankton gradient. The importance of cross-diffusion can be examined through K_{PP}/K_{PN}, the ratio of effective diffusivities from Equation 8, which depends on the ratio of reaction rates, $\lambda/\mu N_D$ (see Text S4 in Supporting Information S1). $\lambda/\mu N_D$ also scales the entrainment terms in the nondimensionalized N and P equations. When $\lambda/\mu N_D \ll 1$, K_{PN} is larger than K_{PP}, that is, the phytoplankton eddy flux is controlled by the mean nutrient gradient. This corresponds to cases where the leading order biological behavior is governed solely by the nonlinear growth term, which explicitly couples N and P. While the specifics of this result depend on the mathematical representation of the biological reaction terms, cross-diffusion in more complex biogeochemical models deserves further examination.

4. Discussion and Conclusions

It is well known that mesoscale and submesoscale processes impact phytoplankton variability (Flierl & McGillicuddy, 2002; Lévy et al., 2012, 2018; Mahadevan, 2016; McGillicuddy, 2016). However, these scales are not resolved in most global climate models. While significant progress has been made in the parameterization of turbulent fluxes for ocean models (D'Asaro et al., 2014; Fox-Kemper et al., 2008; Gent et al., 1995; Visbeck et al., 1997), many subgrid scale processes are still poorly represented (Fox-Kemper et al., 2019; Hamlington et al., 2014; Li et al., 2019; Smith et al., 2016). Biogeochemical tracers pose an added challenge due to nonlinear reactions, which impact their distribution in addition to advection by the flow (Wallhead et al., 2013). Our goal in this study has been to examine the theoretical limitations of eddy diffusion parameterizations for reactive tracers such as nutrients and phytoplankton. Note that in the context of our simulations, eddy flux refers to the advective transport by the time fluctuating velocity rather than a parameterization of subgrid scale processes. However, the multiple scale analysis from Section 2 is more general, and implies that cross-diffusion will also exist in the ensemble and coarse-grained problems.

We find that the efficacy of the parameterized eddy fluxes depends strongly on the ratio of biological and physical timescales, the Damköhler number. At low Da, gradient-diffusion is accurate since the reaction rates are slow enough that the scalar is approximately nonreactive. At high Da, the scalar is reacting faster than diffusion can act on it, so the gradient seen by the turbulence is small. The tracer evolution is primarily governed by the biological reactions, which explicitly couple N and P. Consequently, cross-diffusion can be important in these regimes. At intermediate Da, the tracers are reacting on the same timescales as the background flow, so changes in tracer concentration result from a complex combination of stirring and growth. As a result, the covariance of u' and P', which determines the phytoplankton flux, is not well represented in terms of the mean fields. The parameterization fails in these regimes, regardless of whether cross-diffusion is included. This is not surprising, since $Da \sim \mathcal{O}(1)$ violates the timescale separation condition needed to derive Equations 7 and 8.

Previous studies have proposed an effective diffusivity that varies as a function of the reaction rate (Plumb, 1979; Pasquero, 2005). However, even simple biogeochemical models, such as the one used in this study, can have multiple reaction timescales whose relative magnitudes affect the equilibrium behavior. Furthermore, the reaction-dependent effective diffusivity in Pasquero (2005) was found to be least accurate when $Da \sim \mathcal{O}(1)$. We suggest this is due to the lack of timescale separation rendering gradient diffusion invalid. When the flow and reaction timescales are similar, it may be difficult to improve the accuracy of parameterized fluxes within the eddy diffusion framework, even if modified to account for the reaction timescale as in Pasquero (2005). This result has implications for coarse resolution climate models, since $Da \sim \mathcal{O}(1)$ approximately applies to phytoplankton growth and loss processes at the submesoscale (Smith, 2017). Therefore, there may be large errors associated with applying gradient diffusion to parameterize eddy fluxes of phytoplankton at the submesoscale.

In large Da regimes, we find that the eddy fluxes of P can depend strongly on gradients in N due to the coupling between the phytoplankton and nutrient evolution equations via biological reaction terms.

Incorporating cross-diffusion in our idealized simulations greatly increased the accuracy of the parameterized fluxes when $Da \gg 1$. This is significant since $Da \sim \mathcal{O}(10^2)$ roughly applies to phytoplankton processes at the mesoscale (Smith, 2017). Therefore, including cross-terms in complex models may provide a way to improve the parameterized fluxes of phytoplankton at the mesoscale using information about the large scales only. We note though that any eddy parameterization which assumes locality in space and time is missing fundamental physical effects. As was shown in Manucharyan et al. (2017), the large-scale eddy field has a finite memory of past ocean states. Recent efforts have also incorporated nonlocal effects into eddy parameterizations using an effective diffusivity kernel that depends on the statistics of the flow field (Bhamidipati et al., 2020). Extending these frameworks to reactive tracers is worth investigation given the key role of phytoplankton in marine ecosystems and the global carbon cycle.

Data Availability Statement

The code to run the coupled physical-biological model used in this study can be found at http://doi.org/10.5281/zenodo.4067095.

Acknowledgments
Thanks to D. Balwada, A. Gnanadesikan and an anonymous reviewer for helpful comments. Thanks also to M. Freilich for useful conversations. This work was conducted, in part, at the 2019 Geophysical Fluid Dynamics Program at Woods Hole Oceanographic Institution, which is supported by the National Science Foundation and Office of Naval Research. Special recognition goes to Charlie Doering, who provided valuable insight into this work and unfortunately passed away earlier this year. The authors greatly appreciate his contributions to this study, as well as his kindness, optimism, and tremendous impact on the entire GFD Program. C. J. Prend was also supported by a NSF Graduate Research Fellowship under Grant DGE-1650112. G. R. Flierl was supported partly by NSF grant OCE-1459702. K. M. Smith was supported by the European Research Council under the European Union's Horizon 2020 research and innovation Grant 742480. A. K. Kaminski was supported by NSF grant OCE-1657676.

References

Abraham, E. R. (1998). The generation of plankton patchiness by turbulent stirring. *Nature*, *391*, 577–580. https://doi.org/10.1038/35361
Aumont, O., Ethe, C., Tagliabue, A., Bopp, L., & Gehlen, M. (2015). Pisces-v2: An ocean biogeochemical model for carbon and ecosystem studies. *Geoscientific Model Development*, *8*, 2465–2513. https://doi.org/10.5194/gmd-8-2465-2015
Behrenfeld, M. J., & Boss, E. S. (2014). Resurrecting the ecological underpinnings of ocean plankton blooms. *Annual Review of Marine Science*, *6*, 167–194. https://doi.org/10.1146/annurev-marine-052913-021325
Bhamidipati, N., Souza, A. N., & Flierl, G. R. (2020). Turbulent mixing of a passive scalar in the ocean mixed layer. *Ocean Modelling*, *149*, 101615. https://doi.org/10.1016/j.ocemod.2020.101615
Brentnall, S., Richards, K., & Brindley, J. (2003). Plankton patchiness and its effect on larger-scale productivity. *Journal of Plankton Research*, *25*, 121–140. https://doi.org/10.1093/plankt/25.2.121
Cramer, J. S. (1987). Mean and variance of r^2 in small and moderate samples. *Journal of Econometrics*, *35*, 253–266. https://doi.org/10.1016/0304-4076(87)90027-3
Cushing, D. H. (1975). *Marine ecology and fisheries*. Cambridge University Press.
D'Asaro, E. A., Thomson, J., Shcherbina, A. Y., Harcourt, R. R., Cronin, M. F., Hemer, M. A., & Fox-Kemper, B. (2014). Quantifying upper ocean turbulence driven by surface waves. *Geophysical Research Letters*, *41*, 102–107.
da Silva, C. B., & Pereira, J. C. F. (2007). Analysis of the gradient-diffusion hypothesis in large-eddy simulations based on transport equations. *Physics of Fluids*, *19*, 035106. https://doi.org/10.1063/1.2710284
Denman, K. L. (2003). Modelling plankton ecosystems: Parameterizing complexity. *Progress in Oceanography*, *57*, 429–452. https://doi.org/10.1016/s0079-6611(03)00109-5
Doney, S. C., Lindsay, K., Caldeira, K., Campin, J.-M., Drange, H., Dutay, J.-C., et al. (2004). Evaluating global ocean carbon models: The importance of realistic physics. *Global Biogeochemical Cycles*, *18*, GB3017. https://doi.org/10.1029/2003GB002150
Falkowski, P. G., Ziemann, D., Kolber, Z., & Beinfang, P. K. (1991). Role of eddy pumping in enhancing primary production in the ocean. *Nature*, *352*, 55–58. https://doi.org/10.1038/352055a0
Fasham, M. J. R., Ducklow, H. W., & McKelvie, S. M. (1990). A nitrogen-based model of plankton dynamics in the oceanic mixed layer. *Journal of Marine Research*, *48*, 591–639. https://doi.org/10.1357/002224090784984678
Ferrari, R., & Nikurashin, M. (2010). Suppression of eddy diffusivity across jets in the southern ocean. *Journal of Physical Oceanography*, *40*, 1501–1519. https://doi.org/10.1175/2010jpo4278.1
Flierl, G. R., & Davis, C. S. (1993). Biological effects of gulf stream meandering. *Journal of Marine Research*, *51*, 529–560. https://doi.org/10.1357/0022240933224016
Flierl, G. R., & McGillicuddy, D. J. (2002). Mesoscale and submesoscale physical-biological interactions. *The Sea*, *12*, 113–185.
Fox-Kemper, B., Adcroft, A., Boning, C. W., Chassignet, E. P., Curchitser, E., Danabasoglu, G., et al. (2019). Challenges and prospects in ocean circulation models. *Frontiers in Marine Science*, *6*, 65. https://doi.org/10.3389/fmars.2019.00065
Fox-Kemper, B., Ferrari, R., & Hallberg, R. (2008). Parameterization of mixed layer eddies. Part I: Theory and diagnosis. *Journal of Physical Oceanography*, *38*, 1145–1165. https://doi.org/10.1175/2007jpo3792.1
Franks, P. J. S. (2002). NPZ models of plankton dynamics: Their construction, coupling to physics, and application. *Journal of Oceanography*, *58*(2), 379–387. https://doi.org/10.1023/a:1015874028196
Freilich, M. A., & Mahadevan, A. (2019). Decomposition of vertical velocity for nutrient transport in the upper ocean. *Journal of Physical Oceanography*, *49*(6), 1561–1575. https://doi.org/10.1175/jpo-d-19-0002.1
Gent, P. R., Willebrand, J., McDougall, T. J., & McWilliams, J. C. (1995). Parameterizing eddy-induced tracer transports in ocean circulation models. *Journal of Physical Oceanography*, *25*, 463–474. https://doi.org/10.1175/1520-0485(1995)025<0463:peitti>2.0.co;2
Gower, J. F. R., Denman, K. L., & Holyer, R. L. (1980). Phytoplankton patchiness indicates the fluctuations spectrum of mesoscale oceanic structure. *Nature*, *288*, 157–159. https://doi.org/10.1038/288157a0
Hamlington, P. E., Roekel, P. V., Fox-Kemper, B., Julien, K., & Chini, G. P. (2014). Langmuir-submesoscale interactions: Descriptive analysis of multiscale frontal spin-down simulations. *Journal of Physical Oceanography*, *44*, 2249–2272. https://doi.org/10.1175/jpo-d-13-0139.1
Hodges, B. A., & Rudnick, D. L. (2004). Simple models of steady deep maxima in chlorophyll and biomass. *Deep-Sea Research I: Oceanographic Research Papers*, *51*, 999–1015. https://doi.org/10.1016/j.dsr.2004.02.009
Hodges, B. A., & Rudnick, D. L. (2006). Horizontal variability in chlorophyll fluorescence and potential temperature. *Deep-Sea Research I: Oceanographic Research Papers*, *53*, 1460–1482. https://doi.org/10.1016/j.dsr.2006.06.006
Jenkins, W. J. (1988). Nitrate flux into the euphotic zone near Bermuda. *Nature*, *331*, 521–523. https://doi.org/10.1038/331521a0

Lee, M., Marshall, D., & Williams, R. (1997). On the eddy transfer of tracers: Advective or diffusive? *Journal of Marine Research*, *55*, 483–505. https://doi.org/10.1357/0022240973224346

Lévy, M., Ferrari, R., Franks, P. J. S., Martin, A. P., & Rivière, P. (2012). Bringing physics to life at the submesoscale. *Geophysical Research Letters*, *39*, L14602. https://doi.org/10.1029/2012gl052756

Lévy, M., Franks, P. J. S., & Smith, K. S. (2018). The role of submesoscale currents in structuring marine ecosystems. *Nature Communications*, *9*, 4758. https://doi.org/10.1038/s41467-018-07059-3

Lévy, M., Klein, P., & Treguier, A.-M. (2001). Impact of sub-mesoscale physics on production and subduction of phytoplankton in an oligotrophic regime. *Journal of Marine Research*, *59*, 535–565. https://doi.org/10.1357/002224001762842181

Lévy, M., & Martin, A. P. (2013). The influence of mesoscale and submesoscale heterogeneity on ocean biogeochemical reactions. *Global Biogeochemical Cycles*, *27*, 1139–1150. https://doi.org/10.1002/2012gb004518

Li, Q., Reichl, B. G., Fox-Kemper, B., Adcroft, A. J., Belcher, S. E., Danabasoglu, t., G., et al. (2019). Comparing ocean surface boundary vertical mixing schemes including Langmuir turbulence. *Journal of Advances in Modeling Earth Systems*, *11*, 3545–3592. https://doi.org/10.1029/2019ms001810

Lightstone, M. F., & Raithby, G. D. (2009). On the validity of the gradient diffusion approach as applied to modelling particle dispersion in a turbulent gaseous flow. *Canadian Journal of Chemical Engineering*, *78*, 478–485.

Mahadevan, A. (2016). The impact of submesoscale physics on primary productivity of plankton. *Annual Review of Marine Science*, *8*, 161–184. https://doi.org/10.1146/annurev-marine-010814-015912

Mahadevan, A., & Campbell, J. W. (2002). Biogeochemical patchiness at the sea surface. *Geophysical Research Letters*, *29*, 32-1–32-4. https://doi.org/10.1029/2001GL014116

Manucharyan, G. E., Thompson, A. F., & Spall, M. A. (2017). Eddy memory mode of multidecadal variability in residual-mean ocean circulations with application to the Beaufort gyre. *Journal of Physical Oceanography*, *47*, 855–866. https://doi.org/10.1175/jpo-d-16-0194.1

Martin, A. (2003). Phytoplankton patchiness: The role of lateral stirring and mixing. *Progress in Oceanography*, *57*, 125–174. https://doi.org/10.1016/s0079-6611(03)00085-5

Martin, A., Richards, K., Bracco, A., & Provenzale, A. (2002). Patchy productivity in the open ocean. *Global Biogeochemical Cycles*, *16*, 9-1–9-9. https://doi.org/10.1029/2001GB001449

McGillicuddy, D. J. (2016). Mechanisms of physical-biological-biogeochemical interaction at the oceanic mesoscale. *Annual Review of Marine Science*, *8*, 125–159. https://doi.org/10.1146/annurev-marine-010814-015606

McKiver, W., Neufeld, Z., & Scheuring, I. (2009). Plankton bloom controlled by horizontal stirring. *Nonlinear Processes in Geophysics*, *16*, 623–630. https://doi.org/10.5194/npg-16-623-2009

Mooney, C. J., & Wilson, J. D. (1993). Disagreements between gradient-diffusion and Lagrangian stochastic dispersion models, even for sources near the ground. *Boundary-Layer Meteorology*, *64*, 291–296. https://doi.org/10.1007/bf00708967

Omand, M. M., D'Asaro, E. A., Lee, C. M., Perry, M. J., Briggs, N., Cetinić, C., & Mahadevan, A. (2015). Eddy-driven subduction exports particulate organic carbon from the spring bloom. *Science*, *348*, 222–225. https://doi.org/10.1126/science.1260062

Papanicolaou, G., & Pironneau, O. (1981). On the asymptotic behavior of motion in random flows. In L. Arnold, & R. Lefever (Eds.), *Stochastic nonlinear systems* (pp. 36–41). Springer. https://doi.org/10.1007/978-3-642-68038-0_4

Pasquero, C. (2005). Differential eddy diffusion of biogeochemical tracers. *Geophysical Research Letters*, *32*, L17603. https://doi.org/10.1029/2005GL023662

Pierrehumbert, R. T. (1994). Tracer microstructure in the large-eddy dominated regime. *Chaos, Solitons & Fractals*, *4*, 1091–1110. https://doi.org/10.1016/0960-0779(94)90139-2

Pierrehumbert, R. T. (2000). Lattice models of advection-diffusion. *Chaos*, *10*, 61–74. https://doi.org/10.1063/1.166476

Platt, T., & Sathyendranath, S. (1988). Oceanic primary production: Estimation by remote sensing at local and regional scales. *Science*, *241*, 1613–1620. https://doi.org/10.1126/science.241.4873.1613

Plumb, R. (1979). Eddy fluxes of conserved quantities by small-amplitude waves. *Journal of Atmospheric Science*, *36*, 1699–1704. https://doi.org/10.1175/1520-0469(1979)036<1699:efocqb>2.0.co;2

Richards, K., & Brentnall, S. (2006). The impact of diffusion and stirring on the dynamics of interacting populations. *Journal of Theoretical Biology*, *238*, 340–347. https://doi.org/10.1016/j.jtbi.2005.05.029

Smith, K. M. (2017). *Effects of submesoscale turbulence on reactive tracers in the upper ocean (Unpublished doctoral dissertation)*. University of Colorado Boulder.

Smith, K. M., Hamlington, P. E., & Fox-Kemper, B. (2016). Effects of submesoscale turbulence on ocean tracers. *Journal of Geophysical Research: Oceans*, *121*, 908–933. https://doi.org/10.1002/2015JC011089

Sobel, A. (1999). Diffusion versus nonlocal models of stratospheric mixing, in theory and practice. *Journal of Atmospheric Science*, *56*, 2571–2584. https://doi.org/10.1175/1520-0469(1999)056<2571:dvnmos>2.0.co;2

Srokosz, M., Martin, A., & Fasham, M. (2003). On the role of biological dynamics in plankton patchiness at the mesoscale: An example from the eastern North Atlantic Ocean. *Journal of Marine Research*, *61*, 517–537. https://doi.org/10.1357/002224003322384915

Taniguchi, D. A. A., Franks, P. J. S., & Poulin, F. J. (2014). Planktonic biomass size spectra: An emergent property of size-dependent physiological rates, food web dynamics, and nutrient regimes. *Marine Ecology Progress Series*, *514*, 13–33. https://doi.org/10.3354/meps10968

Taylor, G. I. (1921). Diffusion by continuous movements. *Proceedings of the Royal Society A*, *20*, 196–212.

Turner, E. L., Bruesewitz, D. A., Mooney, R. F., Montagna, P. A., McClelland, J. W., Sadovski, A., & Buskey, E. J. (2014). Comparing performance of five nutrient phytoplankton zooplankton (NPZ) models in coastal lagoons. *Ecological Modelling*, *277*, 13–26. https://doi.org/10.1016/j.ecolmodel.2014.01.007

Tzella, A., & Haynes, P. H. (2007). Small-scale spatial structure in plankton distributions. *Biogeosciences*, *4*, 173–179. https://doi.org/10.5194/bg-4-173-2007

Uchida, T., Balwada, D., Abernathey, R. P., McKinley, G. A., Smith, S. K., & Lévy, M. (2020). Vertical eddy iron fluxes support primary production in the open southern ocean. *Nature Communications*, *11*, 1125. https://doi.org/10.1038/s41467-020-14955-0

Vanag, V. K., & Epstein, I. R. (2009). Cross-diffusion and pattern formation in reaction-diffusion systems. *Physical Chemistry Chemical Physics*, *11*, 897–912. https://doi.org/10.1039/b813825g

Visbeck, M., Marshall, J., Haine, T., & Spall, M. (1997). Specifications of eddy transfer coefficients in coarse-resolution ocean circulation models. *Journal of Physical Oceanography*, *27*, 381–402. https://doi.org/10.1175/1520-0485(1997)027<0381:soetci>2.0.co;2

Wallhead, P. J., Garçon, V. C., & Martin, A. P. (2013). Efficient upscaling of ocean biogeochemistry. *Ocean Modelling*, *63*, 40–55. https://doi.org/10.1016/j.ocemod.2012.12.002

Young, W. R., Roberts, A. J., & Stuhne, G. (2001). Reproductive pair correlations and the clustering of organisms. *Nature*, *412*, 328–331. https://doi.org/10.1038/35085561